1. Materials

All chemicals and solvents were purchased from Sigma Aldrich or SAMCHUN and used without further purification.

2. Experimental procedures

Benzo[1,2-c:3,4-c':5,6-c'']trifuran, 1: The synthesis was performed using a previously reported literature procedure.[1] ^{1}H NMR (300 MHz, $CDCl_3$, 298 K): δ 7.8 (s, 6H, Ar-H).

(1R,4S,5S,8R)-1,4,5,8-Tetrahydro-1,4:5,8-diepoxyanthracene, 2: The synthesis was performed using a previously reported literature procedure.[2] ^{1}H NMR (300 MHz, $CDCl_3$, 298 K): δ 5.63 (d, 4H, OCH), 7.03 (dd, 4H, C=CH), 7.20 (s, 2H, Ar-H).

Cycloocta[1,2-c3,4-c'5,6-c''7,8-c''']tetrafuran, 3: The synthesis was performed using previously reported literature procedure.[S2] ^{1}H NMR (300 MHz, $CDCl_3$, 298 K): δ 7.20 (s, 8H, Ar-H).

2D ep-POP: A mixture of cyclotrifuran **1** (0.0314 g, 0.16 mmol, 1 eq.), diepoxyanthracene **2** (0.05 g, 0.24 mmol, 1.5 eq.) and 2 mL of DMF was placed into an ampoule and then flame-sealed in liquid N_2 under vacuum. The ampoule was transferred to a pre-heated oven at 160^{o}C and kept for 3 d. The resulting powder was filtered and washed with chloroform (50 mL), acetone (50 mL), methanol (50 mL), and water (50 mL). The **2D ep-POP** powder (0.043 g, 53%) was soxhleted in acetone for 5 days and dried under vacuum at 100^{o}C for 6 h. FT-IR (powder): 3056, 2983, 2942, 2362, 2158, 1958, 1663, 1458, 1276, 1001, 1081, 635 cm^{-1}. Anal. calcd. for $C_{33}H_{22}O_6$: C, 77.18; H, 4.12; O, 18.69. Found: C, 76.82; H, 4.91; O, 18.27.

3D ep-POP: The above procedure was followed by using cyclotetrafuran (0.031 g, 0.12 mmol, 1 eq.), **3**, diepoxyanthracene **2** (0.05 g, 0.24 mmol, 2 eq.) and 2 mL of DMF. **3D ep-POP** (0.046 g) was isolated in 54% yield. FT-IR (powder): 2970, 2926, 2855, 1444, 1382, 1336, 1111, 1003, 929, 852, 697, 604 cm^{-1}. Anal. calcd. for $C_{44}H_{28}O_8$: C, 77.18; H, 4.12; O, 18.69. Found: C, 77.13; H, 4.19; O, 18.68.

3. Characterization methods

Characterization. X-ray photoelectron spectroscopy (XPS) analysis was performed with a multi-purpose XPS (Sigma Probe, Thermo VG Scientific, X-ray Source: monochromatic Al K-alpha). Solid-state CP/MAS ^{13}C NMR spectra were obtained using Bruker Avance 400 MHz

NMR instrument. Thermogravimetric analysis (TGA) was performed on a Netzsch-TG 209 F3 at a heating rate of 2°C min^{-1} up to 800°C under air. FT-IR spectra were recorded on Shimatzu IRTracer-100. To obtain the spectra for the activated samples, the polymers were degassed at 100°C for 6 h and the spectra were taken before cooling down to room temperature to avoid adsorption of atmospheric moisture. Powder X-ray diffraction (PXRD) patterns of the polymers with 2θ ranging from 5 to 80° were obtained using a Rigaku D/MAX-2500 Multi-purpose High Power X-ray diffractometer. The morphology of ep-POPs were investigated using a field emission scanning electron microscope (FE-SEM, Sirion) and elemental mappings were performed using energy-dispersive X-ray (EDAX). Elemental compositions of the polymers were investigated using FlashEA 2000 Series [C, H, N] Elemental Analyzer. Ar adsorption and desorption isotherms were measured at 87 K on a Micromeritics 3Flex Surface Characterization Analyzer. All samples were outgassed at 100°C for 6 h prior to the analysis.

Water uptake experiments. Volumetric water uptake experiments were carried out using a Microtrac BEL BELSORP-aqua 3 at 298 and 313 K. All polymer samples were activated to remove residual solvent and water prior to the measurements. The collected isotherm data was fitted in the Clausius-Clapeyron equation in order to calculate isosteric heats of adsorption (Q_{st}) of water. Gravimetric water uptake at various temperatures was measured using a Q5000SA sorption analyzer from TA instruments. Prior to the measurements, the polymers were dehydrated at 80°C with a flow of dry N_2 gas. The temperature was lowered to 5°C. The analysis was proceeded by increasing the temperature up to 45°C with increment of 5°C/min, while maintaining the humidity at 90%. The cycle experiments of gravimetric water uptake were performed using Shimatzu DTG-60A instrument. In order to remove residual solvent and water prior to the experiments, ep-POPs were dried *in-situ* at 100°C. The cycle experiment was performed by using N_2 gas as a carrier gas bubbled through a vessel of deionized water. The total gas flow rate was maintained at 50 cm^3/min for the entire experiment. The temperature range of 25-70 °C was preserved for twenty cycles, with a heating rate of 1°C/min at constant humidity of 90% RH.

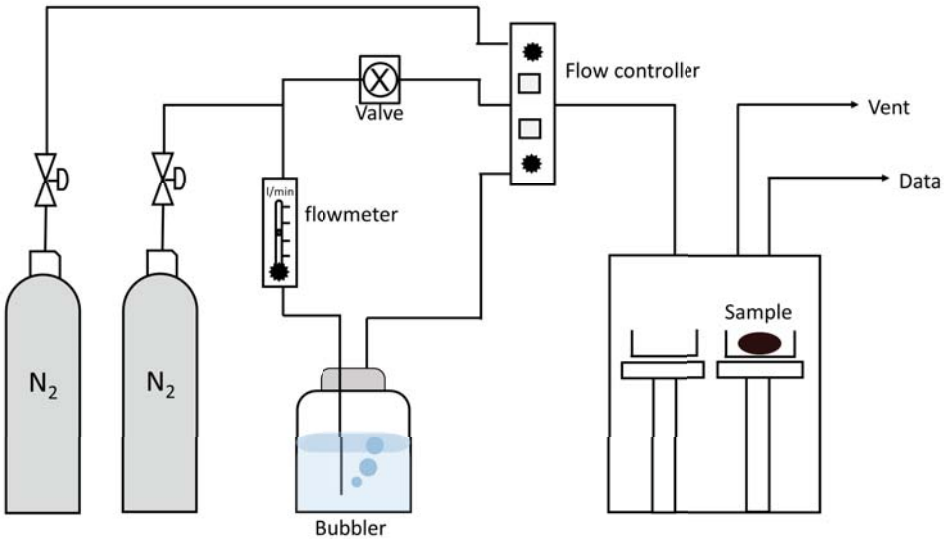

Schematic description of the experimental set-up for the cycle experiments of gravimetric uptake of water using thermogravimetric analysis instrument.

4. Characterization of 2D ep-POP and 3D ep-POP

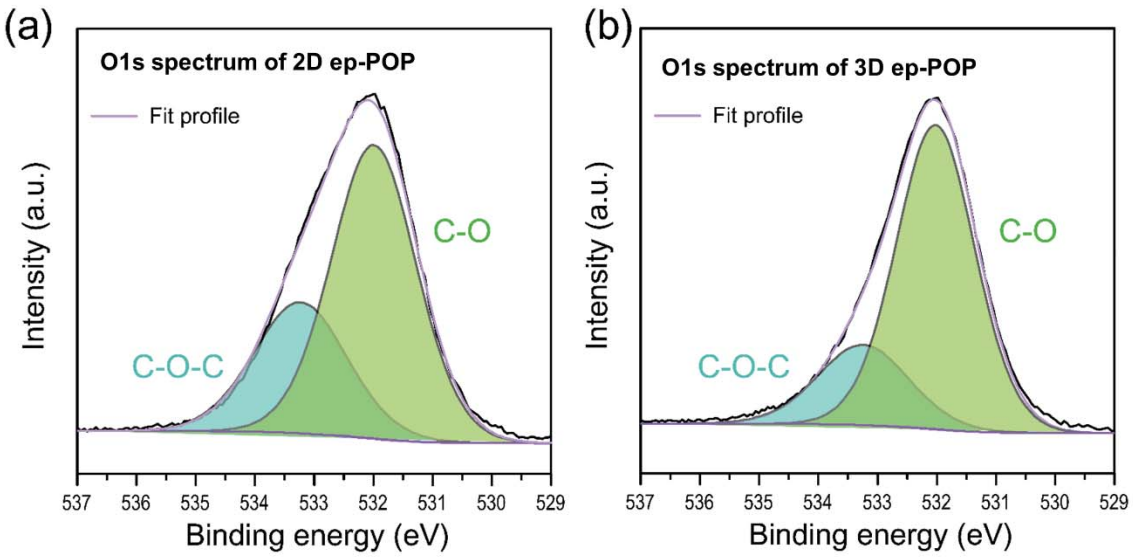

Figure S1. O1s XPS analysis of (s) 2D ep-POP and (b) 3D ep-POP.

Table S1. C 1s binding energy and surface concentration from the XPS spectra of 2D ep-POP and 3D ep-POP.

Binding Energy (eV)	Chemical Bonds	Concentration %	
		2D ep-POP	3D ep-POP
284.5	C=C	71.9	59.9
285.6	C-C	10.8	16.8
286.4	C-O-C / C-O-H	12.2	19.2
288.6	C-O	5.1	4.1

Table S2. O 1s binding energy and surface concentration from the XPS spectra of 2D ep-POP and 3D ep-POP.

Binding Energy (eV)	Chemical Bonds	Concentration %	
		2D ep-POP	3D ep-POP
532.0	C-O-C	67.1	76.3
533.5	O-H	32.9	23.7

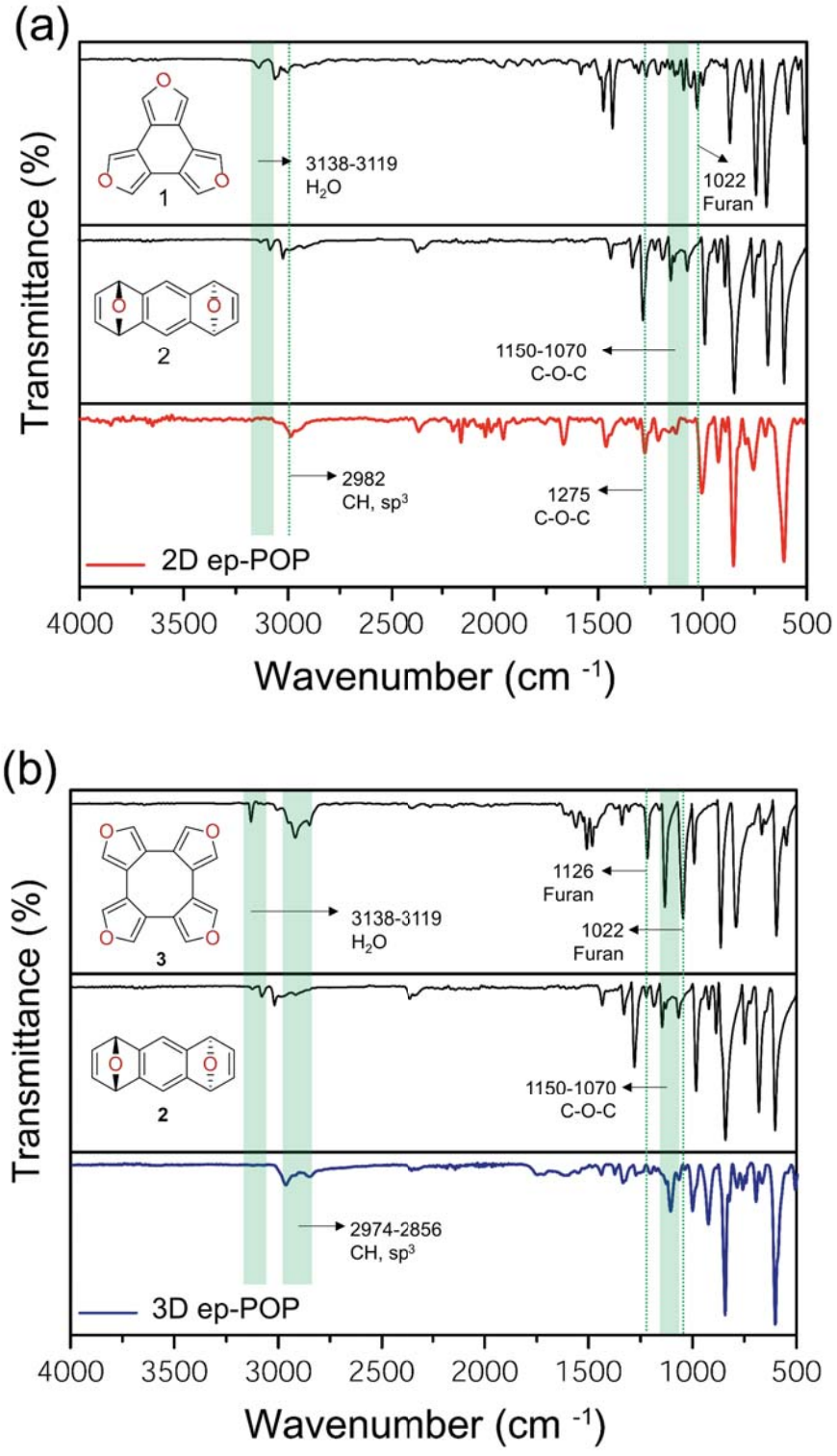

Figure S2. FT-IR spectra of (a) 2D ep-POP and (b) 3D ep-POP.

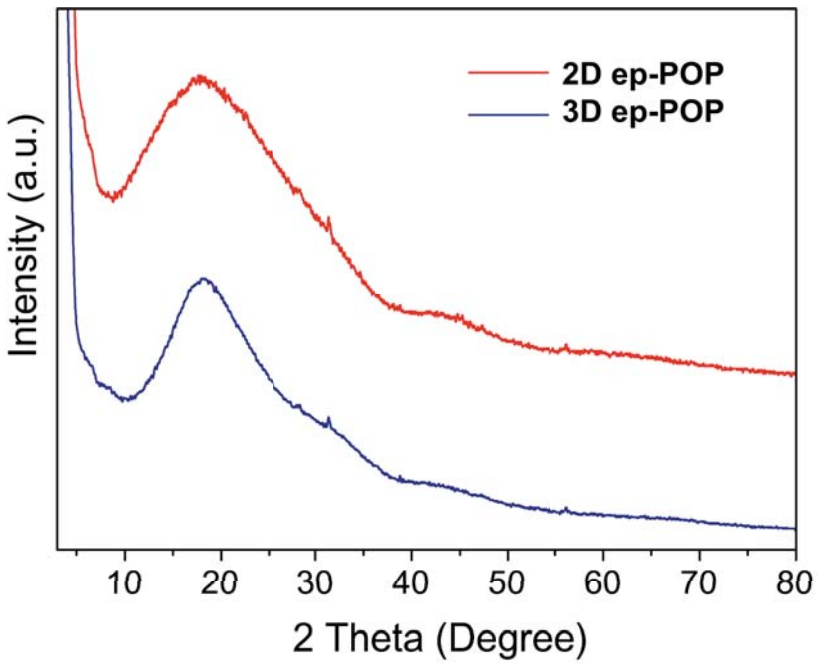

Figure S3. Powder X-ray diffraction (PXRD) patterns of 2D ep-POP and 3D ep-POP in the 2θ range of 3 to 80°, indicating the amorphous nature of resulting polymers.

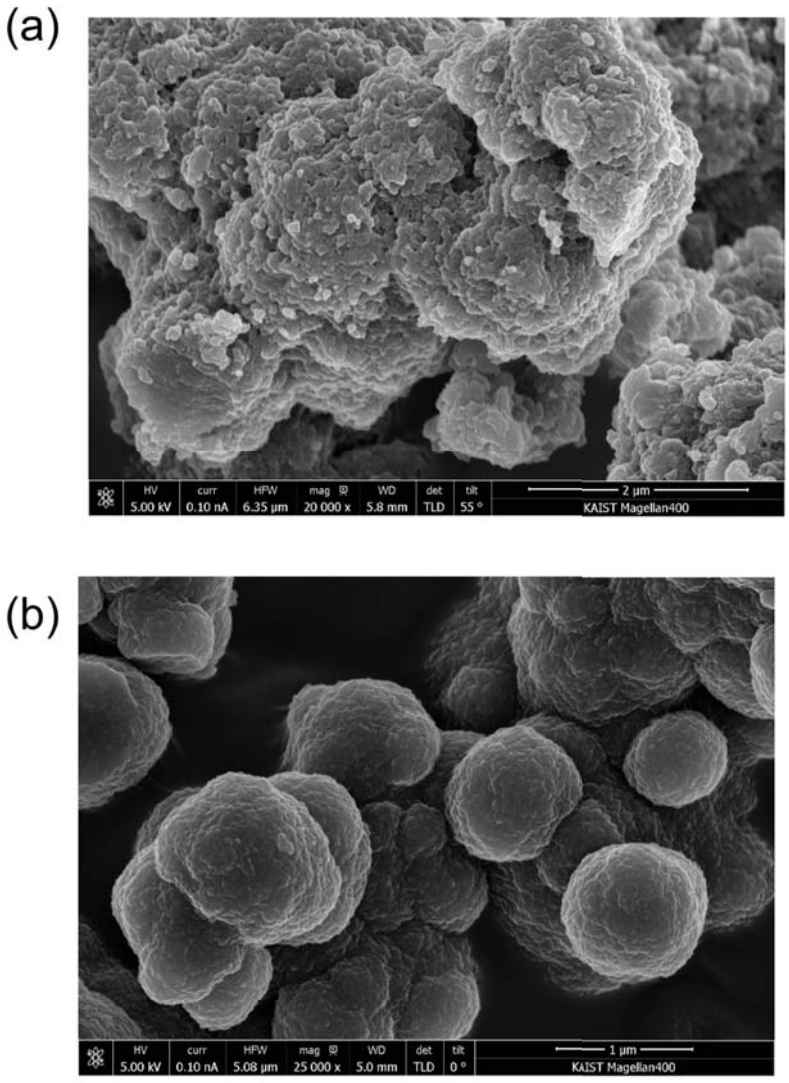

Figure S4. FE-SEM images of (a) 2D ep-POP and (b) 3D ep-POP.

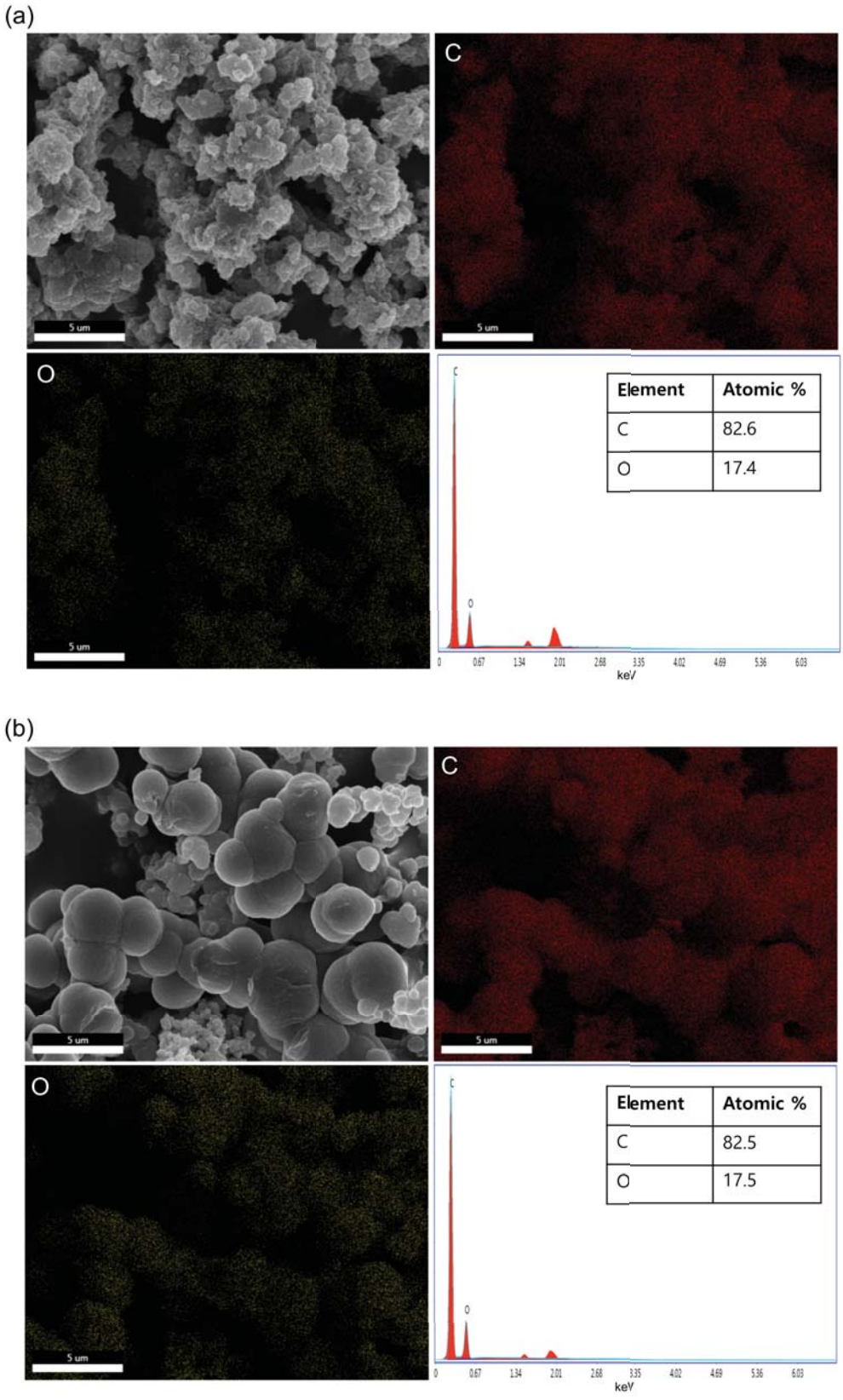

Figure S5. EDS elemental mappings of C/O for (a) 2D ep-POP and (b) 3D ep-POP.

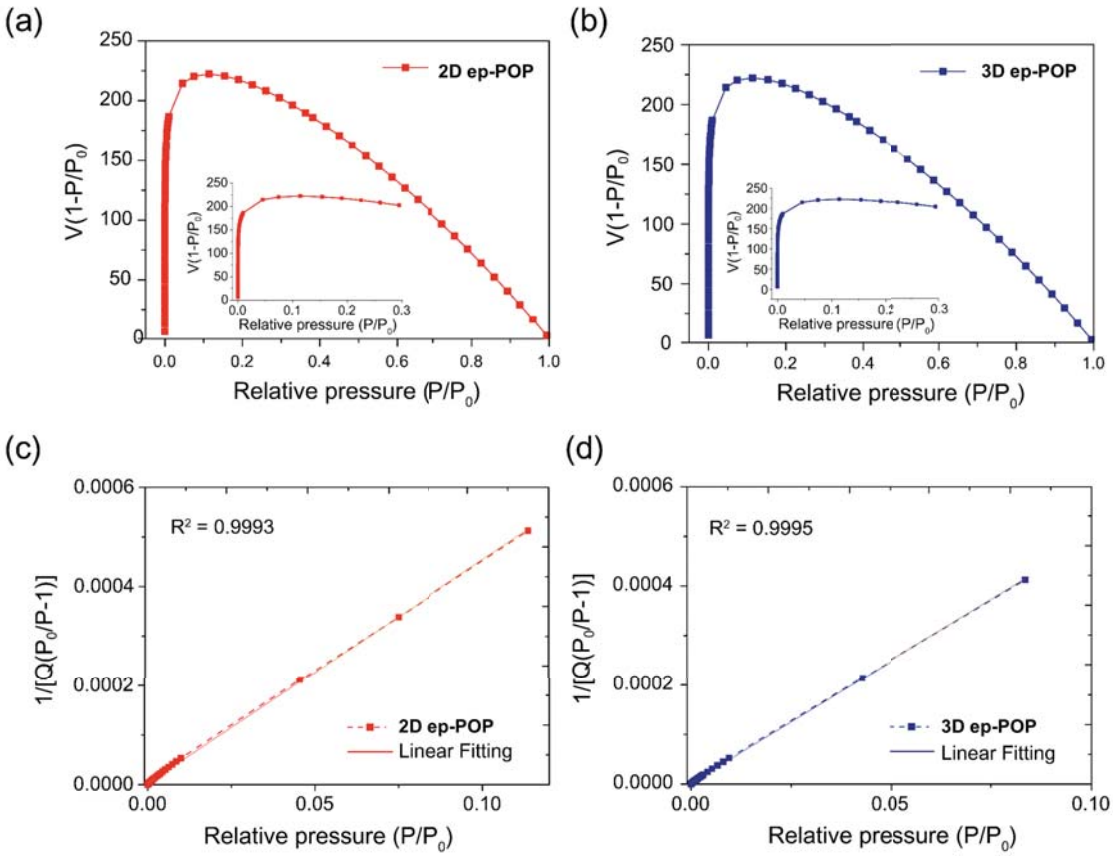

Figure S6. Calculated Rouquerol plots of (a) 2D ep-POP and (b) 3D ep-POP (Inset: Expanded P/P_0 region used for the BET surface area calculations). For surface area calculations, we selected the pressure range where the term $V(1\text{-}P/P_0)$ continuously increases with P/P_0. BET linear plots of (c) 2D ep-POP and (b) 3D ep-POP obtained from Ar isotherms at 87 K.

Table S3. BET surface areas and vapor uptake capacities along with the isosteric heats of adsorption (Q_{st}) values of ep-POPs at zero coverage.

Polymer	S_{BET} ($m^2\ g^{-1}$)	S_{micro} ($m^2\ g^{-1}$)	Langmuir ($m^2\ g^{-1}$)	V_{micro} ($cm^3\ g^{-1}$)	d_{micro} (nm)	H_2O adsorption (wt%)		Q_{st} for H_2O (kJ mol^{-1})
						298 K	313 K	
2D ep-POP	852	464	1049	0.18	0.47	41.1	33.9	48.1
3D ep-POP	779	462	936	0.17	0.40	41.1	26.3	59.6

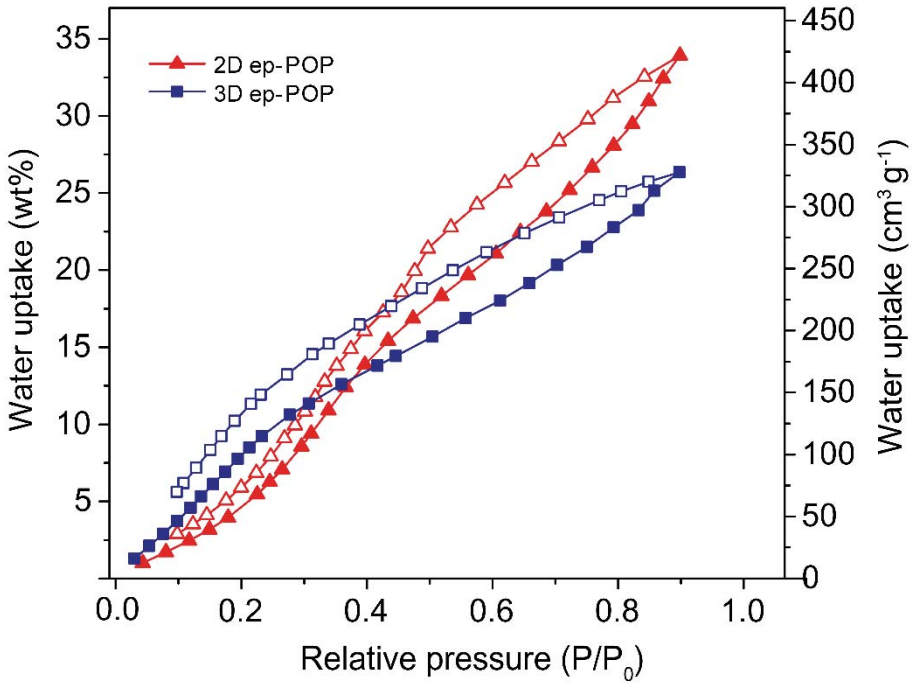

Figure S7. Vapor adsorption isotherms of 2D ep-POP and 3D ep-POP at 313 K. Filled and empty symbols represent vapor adsorption and desorption, respectively.

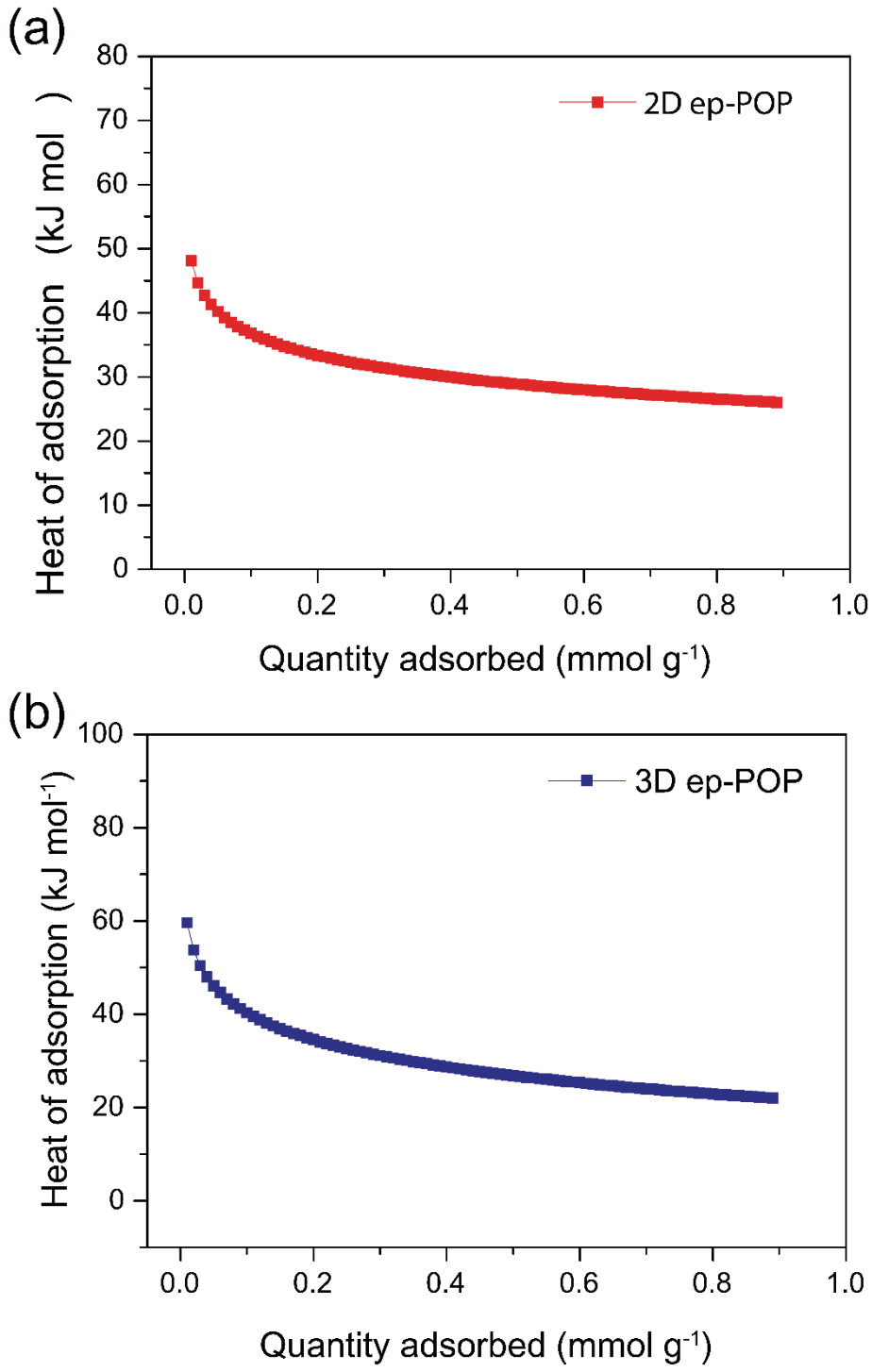

Figure S8. The isosteric heats of adsorption (Q_{st}) of H_2O for 2D and 3D ep-POPs calculated from the Clausius-Clapeyron equation using the adsorption data at 298 and 313 K.

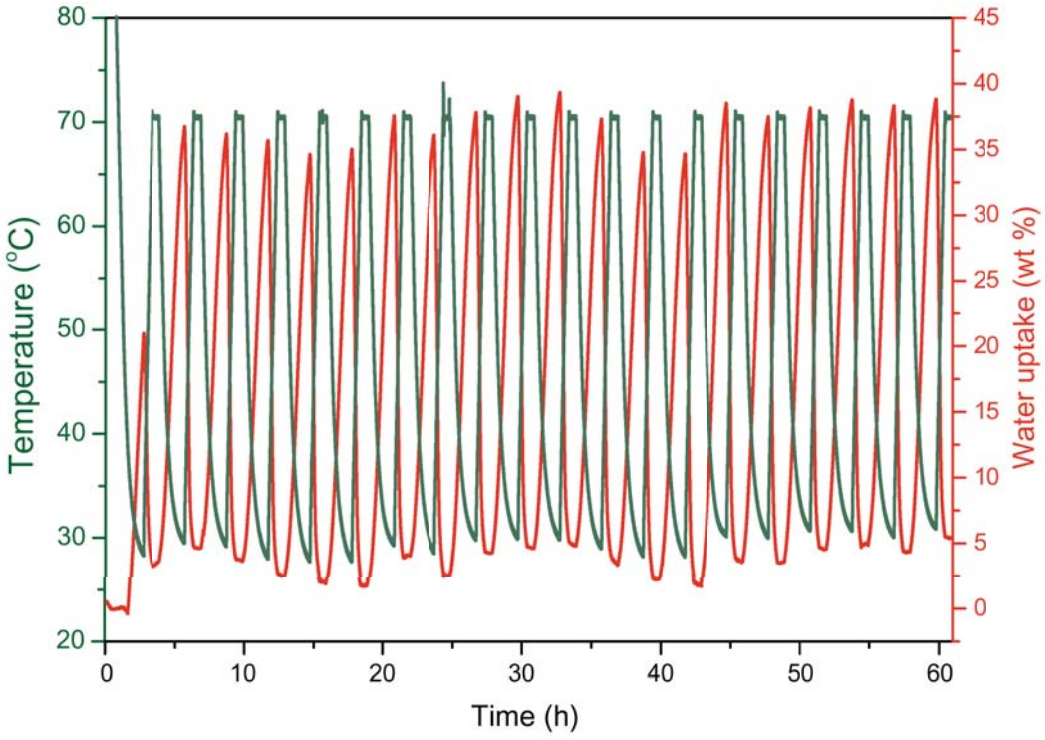

Figure S9. The cycle performance using 2D ep-POP over 40 cycles by the continuous change in temperature between 30 and 70°C at constant humidity of 90% RH.

Table S4. Summary of water uptake capacities of ep-POPs and other representative porous materials at 90% RH.

Adsorbent	H_2O adsorption (wt%)	Measurement temperature (°C)	Ref.
2D ep-POP	42.4 42.3 42.1 41.7 41.2 40.6 40.1 39.7 39.2	5 10 15 20 25 30 35 40 45	**This work**
3D ep-POP	41.3 41.6 41.7 41.4 41.2 40.8 40.5 40.2 39.9	5 10 15 20 25 30 35 40 45	**This work**
Alumina	24 10	20 40	[3]
Basolite A100	37 36	25 40	[4]
Basolite F300	35 40	25 40	[4]
MOF-801-P	42 40	35 45	[5]
RF-100	23 36	5 25	[6]
RF-200	23 39	5 25	[6]
Silica gel	33 30 27	30 35 40	[7]
UiO-66	43	25	[5]
UiO-66-NH_2	40	25	[8]
Zeolite NaA	30 30 30	5 25 40	[9]
Zeolite NaX	28 28 29	10 20 40	[10]

5. References

[1] T. Fallon, A. C. Willis, A. D. Rae, M. N. Paddon-Row, M. S. Sherburn, *Chem. Sci.* **2012**, *3*, 2133-2137.

[2] P. R. Ashton, et al., *J. Am. Chem. Soc.* **1992**, *114*, 6330-6353.

[3] J.-H. Kim, C.-H. Lee, W.-S. Kim, J.-S. Lee, J.-T. Kim, J.-K. Suh, J.-M. Lee, *J. Chem. Eng. Data* **2003**, *48*, 137-141.

[4] S. K. Henninger, F. Jeremias, H. Kummer, C. Janiak, *Eur. J. Inorg. Chem.* **2012**, 2625-2634.

[5] H. Furukawa, F. Gándara, Y.-B. Zhang, J. Jiang, W. L. Queen, M. R. Hudson, O. M. Yaghi, *J. Am. Chem. Soc.* **2014**, *136*, 4369-4381.

[6] T. Horikawa, N. Sakao, D. D. Do, *Carbon* **2013**, *56*, 183-192.

[7] K. C. Ng, H. T. Chua, C. Y. Chung, C. H. Loke, T. Kashiwagi, A. Akisawa, B. B. Saha, *Appl. Therm. Eng.* **2001**, *21*, 1631-1642.

[8] P. M. Schoenecker, C. G. Carson, H. Jasuja, C. J. J. Flemming, K. S. Walton, *Ind. Eng. Chem. Res.* **2012**, *51*, 6513-6519.

[9] K. F. Loughlin, *Adsorption* **2009**, *15*, 337-353.

[10] M. M. Dubinin, V. A. Astakhov in *Molecular Sieve Zeolites-II, Vol. 102*, (Eds.: M. F. Edith, B. S. Leonard), American Chemical Society, Washington, DC, **1971**, pp. 69-85.